

Project Number D4.087.00	Client	Report Number CR 07-020		 SICOMP
Date 2007-04-04	Reference	Revision		
Registered	Issued by Anders Edwall	Checked by KO	Approved by KO	

Failure Load Predictions of Composite Structures during Fire

Anders Edwall

SICOMP AB, Box 271, SE-941 26 Piteå

Abstract

A methodology has been derived for designing composite structures for fire safety. Fire simulation software such as *Com Fire* and *Csp Fire* as well as the FE-software *Ansys* have been tested and validated. Also an *Excel* tool has been created to perform simplified failure load predictions.

Keywords:

Distribution list (only for confidential reports)

Organisation	Name	Copies

All rights reserved. No part of this publication may be reproduced and/or published by print, photoprint, microfilm or any other means without the previous written consent of SICOMP AB. In case this report was drafted on instructions, the rights and obligations are subject to the relevant agreement concluded between the contracting parties. Submitting the report for inspection to parties who have a direct interest is permitted. © 2007 SICOMP AB.

Contents

	Page
1. Introduction	3
2. Literature study	4
2.1. Fire	4
2.2. Blast	7
3. Fire Simulation Software	8
3.1. Com Fire and Csp Fire	8
3.1.1. <i>Theory</i>	8
3.1.2. <i>Simulations</i>	10
4. Thermo-Mechanical Simulation Software	17
4.1. Ansys [18] simulation case 1	17
4.2. Failure load prediction tool	20
4.2.1. <i>Theory</i>	20
4.2.2. <i>Procedure</i>	28
4.2.3. <i>Simulation case 1</i>	29
5. Failure Load Predictions of Composite Structures during Fire	32
5.1. Material Degradation	32
5.1.1. <i>Fiber</i>	32
5.1.2. <i>Matrix</i>	32
5.1.3. <i>Core Material</i>	33
5.2. Failure Hypothesis	33
5.3. Composite Structure with Fire Insulation	34
5.3.1. <i>Procedure</i>	34
5.3.2. <i>Parameter Study</i>	35
5.3.3. <i>Summary</i>	40
5.4. Composite Structure without Fire Insulation	40
5.4.1. <i>Procedure</i>	40
5.4.2. <i>Parameter Study</i>	41
6. Conclusions	44
7. Acknowledgements	45
8. References	45

1. Introduction

Fire response simulations on composite materials gets increasingly important, as the materials are used for load carrying structures, such as in military and commercial ships. Real life fire tests are expensive and classifying a new material for usage can be costly. In this thesis available software tools for predictions of degradation of composite materials subjected to fire have been evaluated. A methodology for designing composite structures that fulfils standards for fire safety on ships and in aerospace has also been proposed. A short literature study was made on the subject of fire safety. There are some who have addressed the problem but few simple tools were found. Two softwares, *Com Fire* and *Csp Fire*, for simulating fire in composites were evaluated and a methodology for predicting failure was developed with those softwares together with a tool developed in Microsoft *Excel*. Also the possibility to use FE-software such as *Ansys* was evaluated for simulating fire. Both methods were compared to measured data, with good resulting agreement.

2. Literature study

A literature study has been carried out in two different areas concerned with fire simulation in composites.

2.1. Fire

The fire resistance of polymer resins can be improved with various additives, such as alumina trihydrate (ATH). By adding 60 parts ATH by weight to 100 parts polyester the time to ignition will be significantly longer while heat release and smoke development is lowered [1]. Disadvantages with adding this large amount of additives are not only decreases in mechanical performance but also a more complicated manufacturing. Halogenated resins do not have the same disadvantages regarding lowered processability and mechanical properties, they can however produce toxic and corrosive smoke and are only suitable for external parts of the superstructure. In Ref. (1) two halogenated resins are examined, chlorinated polyester and brominated vinylester. Time to ignition for the polyester resin is only slightly shorter than with ATH additive while for the brominated vinylester it is shorter than for standard vinylester. Heat release is lower for both halogenated resins while smoke development is slightly higher than for the standard resins.

A simple model for predicting time to failure for composite single skin panels exposed to fire is found in Ref. (2) and (3). A temperature gradient in the material is assumed and thereby a corresponding property gradient

$$X = Ax^2 + Bx + C \quad (1)$$

where

$$A = \frac{2\Delta - 4\Delta_1}{h^2}, \quad B = \frac{4\Delta_1 - \Delta}{h},$$

$$C = E_1, \quad \Delta = E_2 - E_1, \quad \Delta_1 = E_c - E_1.$$

- x = through thickness coordinate
- h = thickness of plate
- E1 = Elastic modulus at hot face
- E2 = Elastic modulus at cold face
- Ec = Elastic modulus at center of laminate

An experimental/theoretical work is later presented [2]. An ideal property degradation curve fitted to experimentally obtained data was used. It is assumed that all components of the elasticity tensor follow this master degradation curve. A 3D thermal analysis was made to get the temperature distribution in the laminate and with the fitted degradation curve the material degradation distribution could be obtained.

Criteria for failure are not clearly described, “In the context of these simulations failure occurs when out-of-plane displacement under the fixed loads becomes unbounded.”

Laminates were manufactured with resin transfer moulding, RTM, with thermocouples co-moulded in at various locations so that the temperature distribution could be measured during the fire test. A test jig was built with two hydraulic rams located on the top for applying in-plane loading and a third ram applying out-of-plane loading at the cold face. The jig is bolted onto the rim of a furnace for fire exposure. Plate thickness was 12.2 mm and height and width was 914 mm and 711 mm respectively.

A standard thermal analysis combined with the same fitted property degradation curve as mentioned above was done and the resultant property degradation distribution was used in structural analysis.

Simulations and predicted failure time was compared to the experimental results. The predicted failure time was between 75 and 80 minutes while the failure time from the experimental result was 65 minutes. The writer notes that the degradation curve was approximately obtained, while also the thermocouples embedded in the material, form induced defects. This could help to explain why the predicted time is longer.

In Ref. (4) a study has been made on the post-fire properties of glassfiber/polyester composites. The tests show a significant reduction in tensile and inter laminar shear properties. The loss of properties was assumed to be caused by charring and delamination. A thermal barrier in form of intumescent paint or insulation in form of a fiber mat reduced the degradation considerably. Furthermore analytical models are presented for predicting the reduction in failure load.

A thermo-viscoplastic model for rate-dependent and temperature-dependent behaviour is presented in Ref. (5). The model is compared to experimental data on PEEK and vinylester with good agreement. The glassfiber/polyester composite was only strain dependent at temperatures below T_g while the AS4/PEEK composite was dependent above and below. The proposed model is

$$\bar{\dot{\epsilon}}^p = B_0 (\bar{\epsilon}^p)^\alpha (\bar{\sigma})^\beta e^{-Q/RT} \quad (2)$$

Where $\bar{\dot{\epsilon}}^p$ is the strain rate, $\bar{\epsilon}^p$ is effective viscoplastic strain, $\bar{\sigma}$ is the effective stress, Q is the activation energy, R the universal gas constant and T the temperature. B , α and β are parameters to be determined from experimental data.

Intumescent coatings are used to protect structures from fire. When subjected to fire the material swells to a porous char and forms a barrier for the heat transfer into the virgin material underneath. A mathematical model for the decomposition of intumescent coatings is presented in Ref. (6) which include mechanisms such as swelling and bubbling.

An analysis of deformation and stresses in a sandwich panel subjected to an elevated temperature such as a fire is presented in Ref. (7). The panel is a sandwich supported on all four edges which is prevented from in-plane displacements. Numerical results are obtained using a simplified quasi-static approach to calculate a distribution of temperature through the thickness. The results are in good agreement with the available experimental data. Thicker faces have little effect on the temperature distribution through the laminate which was explained by the difference in thermal conductivities between the laminate and core.

A potassium aluminosilicate geopolymer composite was evaluated in fire test for ignitability, heat release and smoke development and was compared to a phenolic composite in Ref. (8). Results show that the geopolymer didn't release any smoke or heat and is not ignitable. After being exposed to a 25 kWm^{-2} radiant heat source for 20 minutes the composite was tested in a universal testing machine. The composite retained 67 % of its original flexural strength.

Phenolic is considered as a fire resistant polymer because of its response to fire. Compared to common polymer resins such as polyester and vinylester, the phenolic resin produces less smoke and char. However results from the post fire mechanical testing [9] revealed that the glassfiber/phenolic composite could lose up to 30 % of its original stiffness and strength before any signs of charring could be noticed. This was explained with partial chemical degradation within the matrix. When the material started to char, it had lost up to 70 % of its stiffness and strength.

When polymer composites are exposed to fire, toxic smoke and combustible gases are released. A study on phosphor additive in aerospace epoxy as a retardant was made in Ref. (10). The recommended concentration is ~1.5 % which does not affect the mechanical properties of the epoxy. Results show that the additive promotes charring in the epoxy and in that way flaming and release of gas is retarded. The phosphor itself does not form char, instead it seems to be working as a catalyst in the charring process.

2.2. Blast

A study on how stitching of fibers in a glassfiber/vinylester composite improves the resistance to ballistic projectiles and explosive blasts is presented in Ref. (11). The stitched composites were impacted with a projectile or an underwater blast. Results show that the stitching reduced the amount of damage from the projectile and had a large effect on the explosive blast resistance.

A nonlinear FE-analysis was made using the *Nastran* finite element software on the response of composite panels and is presented in Ref. (12). Models were built in both *Nastran* code and by using the method of modal superposition. Mainly simply supported isotropic laminates was considered but also the case when a blast loaded plate impacts a neighbouring plate. The solution accounts for large plate deflections, plasticity and plate to plate contact. A *Fortran* program is presented which automates the application of a blast load to a finite element mesh. Good agreement was found between the two methods and comparison has been made with experimental data found in literature. However the writer point out that the *Fortran* program is not verified against experimental data.

A methodology has been developed for determining the dynamic response to a blast wave load in composite structures in Ref. (13). The methodology consists of dynamic modelling and progressive failure modelling. Failure modes such as matrix cracking, fiber breakage and fiber/matrix shearing are considered and adopted into the stiffness matrix in every time step.

In [14] the problems with bombs detonated in an airplane are studied. Very little explosives are needed to knock out a large passenger plane. Work is being done on improving the detection of explosives in both checked- and hand-baggage. But it cannot be guaranteed that a small explosive device cannot get through security. This is why work has been done on blast protected baggage containers, made out of composites for light weight.

3. Fire Simulation Software

3.1. Com Fire and Csp Fire

The first two softwares, *Com Fire* [15] and *Csp Fire* [16] are being developed at the University of Newcastle and are used to predict thermal responses in a FRP (fiber reinforced plastic) laminate and SFRP (sandwich fiber reinforced plastic) sandwich laminate respectively, subjected to various defined heat sources.

3.1.1. Theory

In the thermal model used in the two softwares,

$$(\rho C_p)_{com} \frac{\partial T}{\partial t} = \frac{\partial}{\partial x} \left(k_{com} \frac{\partial T}{\partial x} \right) + \dot{M}_g C_{pg} \left(\frac{\partial T}{\partial x} \right) - \frac{\partial \rho_{com}}{\partial t} (Q_p + h_{com} - h_g) \quad (3)$$

$$\text{the term } (\rho C_p)_{com} \frac{\partial T}{\partial t}, \quad (4)$$

where ρ is the density and C_p is the specific heat of the FRP, describes the heat energy transfer in the trough thickness direction [17]. The three terms on the right hand side describes the heat conduction, the energy flux due to gas flux and the energy flux due to decomposition of the resin respectively. The degradation is an endothermic process and will cool the surrounding material as the material degrades.

The decomposition of the material is described with an Arrhenius equation

$$\frac{\partial m}{\partial t} = -A m_0 \left[\frac{m - m_f}{m_0} \right]^n \exp(-E / RT) \quad (5)$$

where

- m = mass of the resin (kg),
- m_0 = initial mass of the resin (kg),
- m_f = final mass of the resin at the end of decomposition (kg),
- A = pre-exponential factor (1/sec),

- T = temperature of the resin (K),
 n = order of the chemical reaction (non-dimensional real),
 E = activation energy (J/mole),
 R = gas constant (= 8.314 J/mole/K).

Equations (3) and (5) are solved simultaneously.

The simulation is done with 1D finite difference in the through thickness direction. The laminate is modelled with 51 nodes forming 50 elements.

The heat flux, q , absorbed by the hot face of the laminate is described by

$$q = \sigma (\epsilon_s \alpha_m T_s^4 - \epsilon_m T_k^4) + h_{nc} (T_{sc} - T_c) \quad (6)$$

where

- q = heat flux absorbed by the hot face of the sample (W/m²);
 T_{sc} = surrounding temperature of heating source (°C);
 T_c = temperature on hot face of the sample (°C);
 T_s = surrounding temperature of heating source (K);
 T_k = temperature on hot face of the sample (K);
 h_{nc} = heat transfer coefficient through natural convection (W/m²/C);
 ϵ_s = emissivity of heating source (-);
 α_m = absorptivity of the HF (hot face) material of the sample (-);
 ϵ_m = emissivity of the HF material of the sample (-);
 σ = Stefan-Boltzmann constant (56.7×10^{-12} W/m²/K⁴).

Throughout this thesis work a value of 0.9 for emissivity, ϵ_s , and 0.8 both for emissivity, ϵ_m , and absorptivity, α_m , of the laminate are used.

The thermal properties of the laminate are calculated with the Rule of Mixture. This is done at each node and time step, to account for the changes due to resin decomposition.

$$(C_p)_{com} = \frac{((C_p)_f \rho_f V_f + (C_p)_m \rho_m V_m)}{(\rho_f V_f + \rho_m V_m)} \quad (7)$$

Where V is the volume fraction, ρ the density and C is the specific heat. Subscript *com*, *f* and *m* denotes composite, fibre and matrix, respectively.

Both softwares ignore the variation of thermal properties with rising temperature in the resin. However in *Com Fire* it is possible to manually feed experimentally obtained data into input files (unit 33 and unit 34).

3.1.2. Simulations

Five cases were prepared for comparison between the two softwares. *Com Fire* [15] only handles single GRP skins while *Csp Fire* [16] handles sandwich material. The cases were designed to work in both softwares. The same model is used in the two softwares so the output should be identical. Input files for the eight cases are explained below.

1. 8 mm thick E-glass/Polyester GRP with thermally insulated cold face:

Com Fire features the option to define boundary conditions on the cold face of the GRP in the input file. A thermal insulation was selected and to get the same condition in *Csp Fire*, the thermal properties of the balsa core input were changed in order to get same properties. The input files for the two softwares are shown in Fig. 1 and 2.

```

8 mm thick EG/PE laminate exposed to standard HC fire.
0.05
20.0
1
1
60.0 8.0 0.42
1 2 11 21 31 41 51
1
1
0.25E+04 0.58E+05 2344600.0
0 1 0
0.9 0.8 0.8
0
0
    
```

Figure 1. The input data file for *Com Fire*.

```

An (8+50+8)mm EG/PE sandwich panel exposed to a HC fire.
0.05
20.0
1000
60.0
Properties of the double GRP skins
1
1
8.0 0.42
1 2 11 21 31 41 51
0.25E+04 0.58E+05 2344600.0
0.0
Properties of the end-grain balsa core
250.0 52.75
50.0
0.0000 0.0000
1180.0 2007.0
0.0
6.5
0.4918E+04 0.6885E+05 1256000.0
1005.0
Thermal boundary conditions on both surfaces
0 1 0
0.9
0.8 0.8
    
```

Figure 2. The input data file for *Csp Fire*.

2. 8 mm thick E-glass/Vinyl Ester GRP with thermally insulated cold face:

The same input data as in test 1 except for change of resin type from polyester to vinylester. This test was done to exclude the polyester material model as the cause of any possible mismatch.

3. 8 mm thick E-glass/Vinyl Ester GRP with balsa core:

Com Fire features the option to define a plate connected to the cold face of the GRP. This was given the same thermal properties as the balsa core in *Csp Fire*. Up to the point where decomposition of the balsa core starts the systems should behave identically.

4. 8 mm thick E-glass/Polyester GRP with thermally insulated cold face:

This is the same laminate as test 1, exposed to a SOLAS (International Convention for the Safety of Life at Sea)-curve heat source which is a defined temperature-time curve.

5. 8 mm thick E-glass/Vinyl Ester GRP with thermally insulated cold face:

In this test a heat source with a constant temperature of 200 °C was applied to the GRP.

6. 8 mm thick E-glass/Vinyl Ester GRP with thermally insulated cold face:

In this test run the balsa core thickness is set to almost zero while the thermal conductivity is set very high simulating a single skin laminate. A core thickness of 0.1 mm was used along with a thermal conductivity of 1.0 W/mK. However this causes the software to crash after a number of time steps depending on the values used. The larger thickness and lower thermal conductivity the more time steps are calculated before crashing. With 0.1 mm thickness and a thermal conductivity of 1.0 W/mK the software crashes after time step 2814.

7. 8 mm thick E-glass/Polyester, without degradation effect:

In this test in *Com Fire* KDEGRA and KMASFL are set to zero. In *Csp Fire* these options are not available but the preexponential factor A is set to zero, ruling out mass changes in the simulation.

8. 12 mm thick E-glass/Vinyl Ester GRP with thermally insulated cold face:

The balsa core was given the same thermal properties as the GRP skins. In that way a 4+4+4 mm GRP laminate was simulated. In *Com Fire* simulations was made with a 12 mm GRP skin.

The cases where simulated and the output are compared below. Big differences were apparent in the output data as shown in the figures below, see Fig. 3.

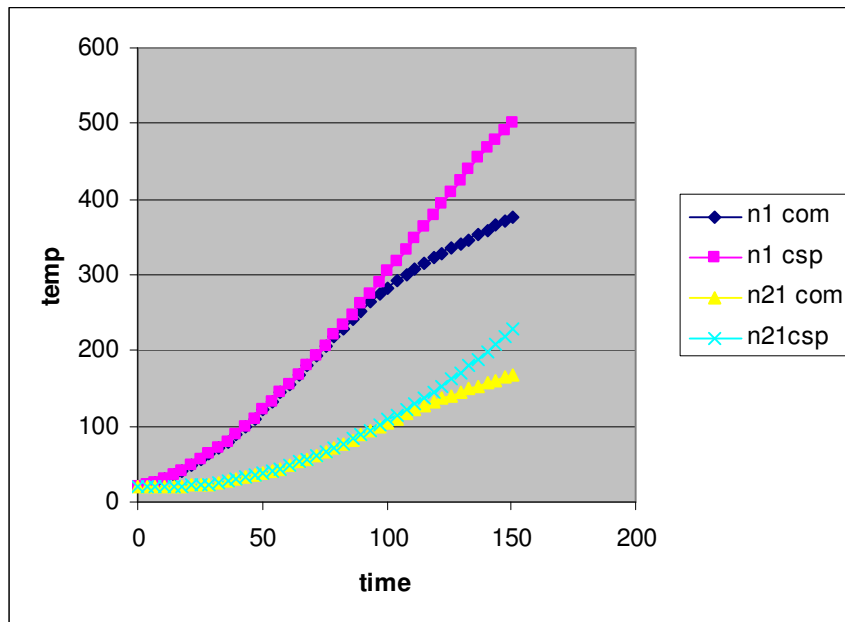


Figure 3. Plotted data from test 1 shows a big difference at elevated temperatures. Temperature at node 1 and 21 in *Com Fire* and *Csp Fire*.

At elevated temperatures the predicted heat transfer in the composite differs in the two softwares. The probable cause of the differences are some bugs in the software code in one or both of the softwares since the model for degradation and heat conductivity used are the same. As can be seen in data from test 2, see Fig. 4, the type of resin does not affect the difference.

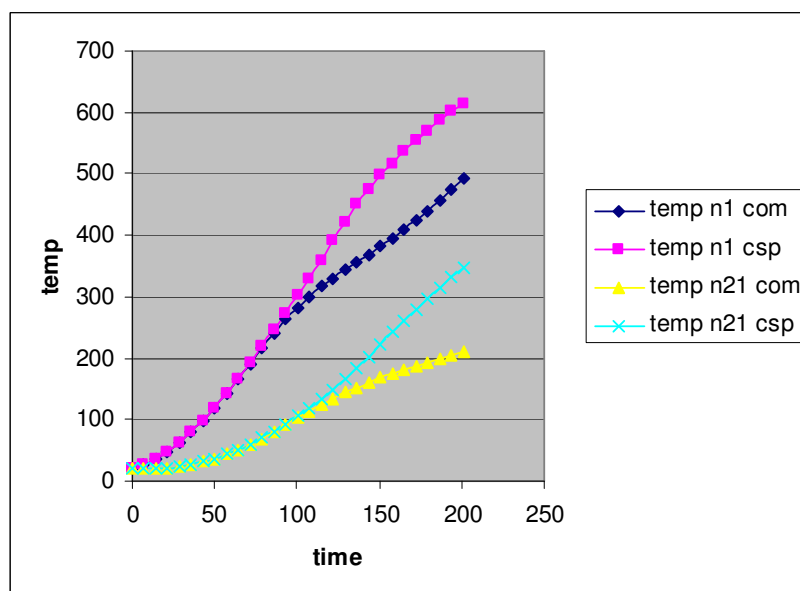


Figure 4. Plotted data from test 2. Temperature at node 1 and 21 in *Com Fire* and *Csp Fire*.

The third test was done only to make sure that the manipulation of the balsa core properties, is not the cause of the mismatch in predictions. As can be seen in Fig. 5 the effects of the core on the temperatures are very small compared to test 2.

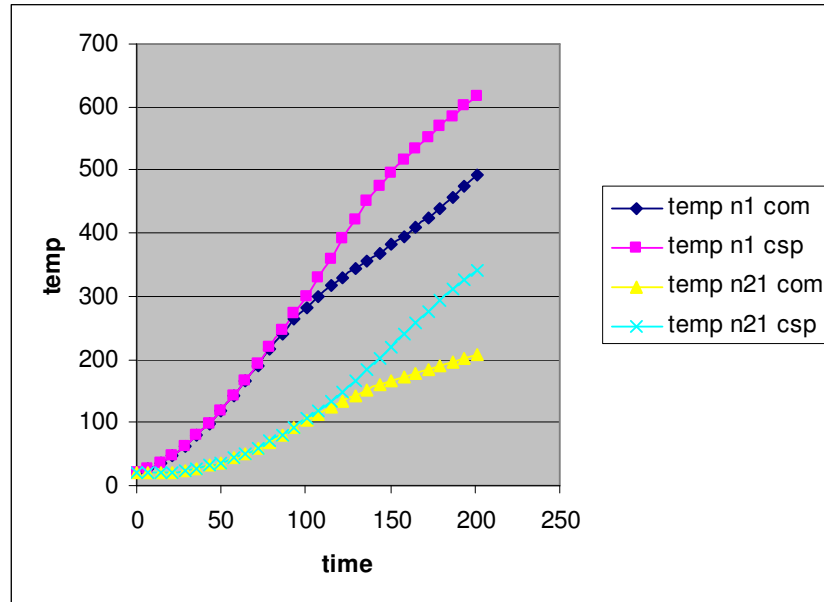


Figure 5. Plotted data from test 3. Temperature at node 1 and 21 in *Com Fire* and *Csp Fire*.

In test 4 where the temperature at the hot surface is defined as a function of time, the difference in heat conduction within the GRP becomes obvious as seen in Fig. 6.

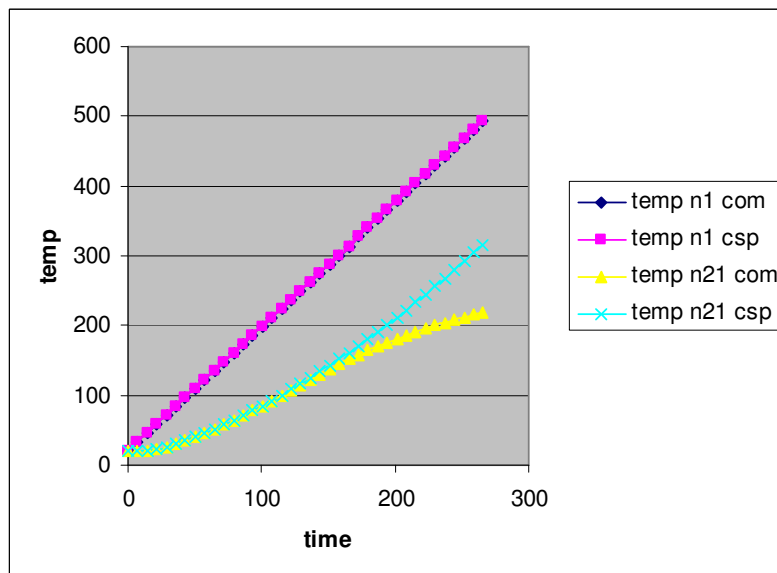


Figure 6. Plotted data from test 4. Temperature at node 1 and 21 in *Com Fire* and *Csp Fire*.

In test 5 a low temperature heat source was used and here we clearly can see that at low temperatures the output data from the two softwares corresponds well, see Fig. 7. When resin degradation and mass flow effects are not included in the simulation the output is identical, see Fig. 8. This is a clear indication that one or both of the softwares have a faulty material degradation model in the code.

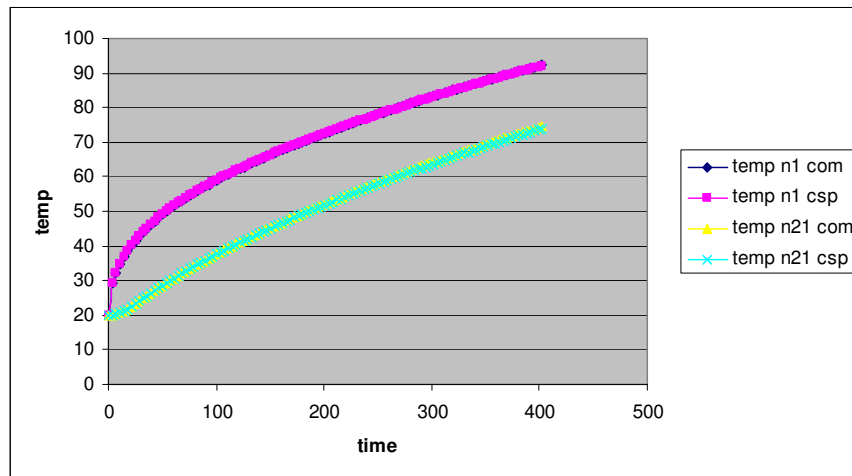


Figure 7. Plotted data from test 5. Temperature at node 1 and 21 in Com Fire and Csp Fire.

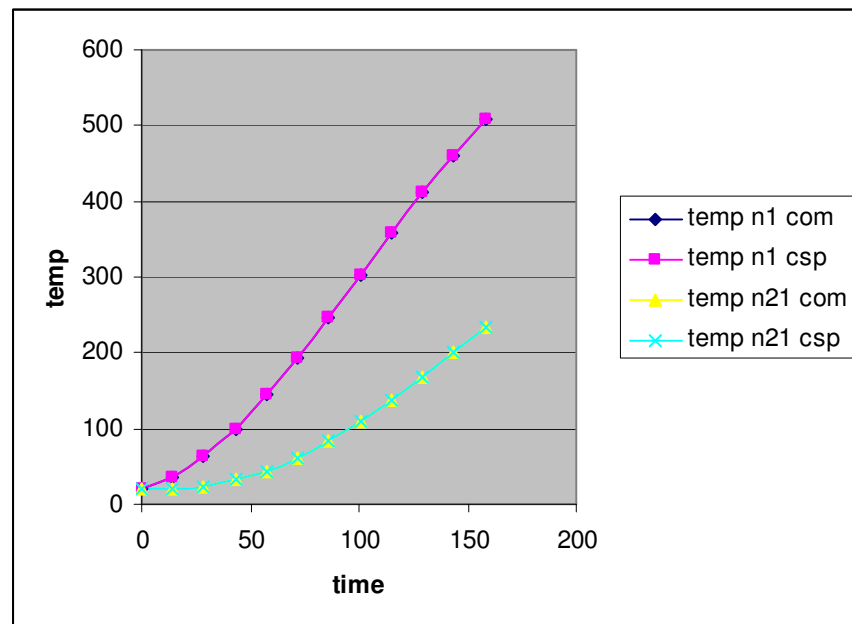


Figure 8. Plotted data from test 7. Temperature at node 1 and 21 in Com Fire and Csp Fire.

Several simulations were made with varying values for activation energy EE , pre-exponential factor AA , and heat of decomposition, H observing what effect each input had on the output. Here it is obvious that the two softwares don't correlate. It is assumed that the *Csp Fire* code is not correct and should not be used in its current state. This assumption is made on the facts that 1: *Com Fire* is more rigorously tested in the past and 2: responses from the different parameters in *Csp Fire* seem to differ from the expected, for example the value for heat of decomposition seems to have no effect at all.

Continued work with *Csp Fire* will only be simulation of thermal heat transfer and all degradation simulations must be done in *Com Fire*. It should be noted that both softwares but especially *Csp Fire* are unstable. Varying parameters too much in either way can cause a very long calculation time or a software crash. An example is when the skins are thin compared to the core. This problem is probably caused by the difference in element size.

4. Thermo-Mechanical Simulation Software

4.1. Ansys [18] simulation case 1

A FE-method was devised for making structural simulations. The calculations are made in two steps. First a thermal analysis is made. For this the thermal material properties are assigned to the different materials in the structure. The load is applied as a temperature on the fire exposed surface of the insulation layer. The temperature varies with time and is derived from a real fire test.

The obtained temperature distribution in the through thickness direction is used along with a set of conditions for softening of the materials. New elastic properties for the sandwich structure can hence be obtained at each time step. In this case a simple set of conditions was used. When the GRP skin reaches T_g the matrix is assumed to loose 99 % of its elastic properties and will stay unchanged at higher temperatures. Next the structural problem is solved through time with a new set of material properties for each time step.

A model was created of a sandwich structure with a stiffener. The sandwich has glass fibre reinforced plastic, GRP, faces which are 2 mm thick. The core is 60 mm thick PVC foam. The stiffener is built up as a sandwich structure which is 60 mm wide. Here the faces are 8.7 mm thick and the core is 220 mm. The whole structure is covered with an 80 mm thick layer of fire insulation. Symmetry is used in two directions to minimize the calculation time, see Fig. 10. The polyester matrix has a T_g of 75 °C and the thermal stability of the PVC core is assumed to be lost at 80 °C.

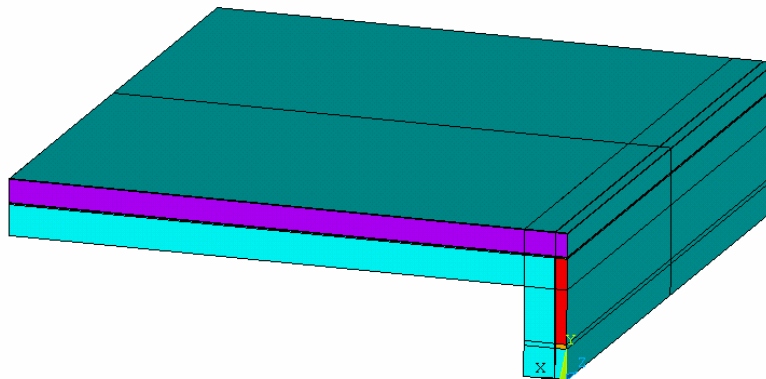


Figure 9. A quarter of the sandwich structure and stiffener. Symmetry is used in x and z-direction.

The simulation will be more accurate when smaller finite elements are used. However more elements makes the calculation time larger. In this simulation, hardware limitations made it not possible to use a finer mesh. The elements are stretched to keep the number of elements down, while still keeping a sufficient resolution in the through thickness direction for the thermal solution, as can be seen in Fig. 10.

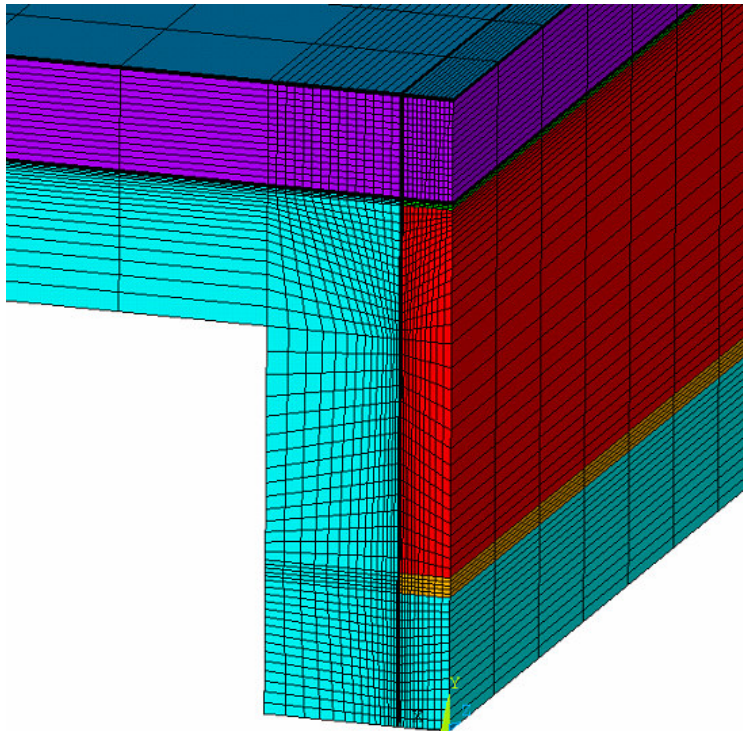


Figure 10. The meshed sandwich structure with insulation. The elements are stretched which is not preferable however necessary to keep the calculation time low, while having enough elements in the through thickness direction.

The boundary conditions for the thermal solution are derived from a real life test and are inserted as a temperature on the surface of the insulation. The model is solved for nodal temperatures, the temperature in every element at each time step. This data is fed into the mechanical solution. When the mean temperature in an element exceeds a preset value the elastic properties of the matrix or the foam core is lowered by a factor of 0.01. This is a good estimation on the reduction of local matrix modulus. The tensile modulus of the laminate is only reduced by 30 % since the fiber properties are dominant, however the compressive modulus is affected in a much larger manner and can be reduced with up to 100 %. The reduction of the local core stiffness is probably lower in reality. The influence of local core stiffness on the global stiffness is however quite small.

Loads are applied as two out of plane forces which are applied at 25 % of the panel length, in from the edges. The forces are evenly distributed across the width as two bands. The panel is simply supported on the two edges perpendicular to the stiffener, the other two are free, see Fig. 11.

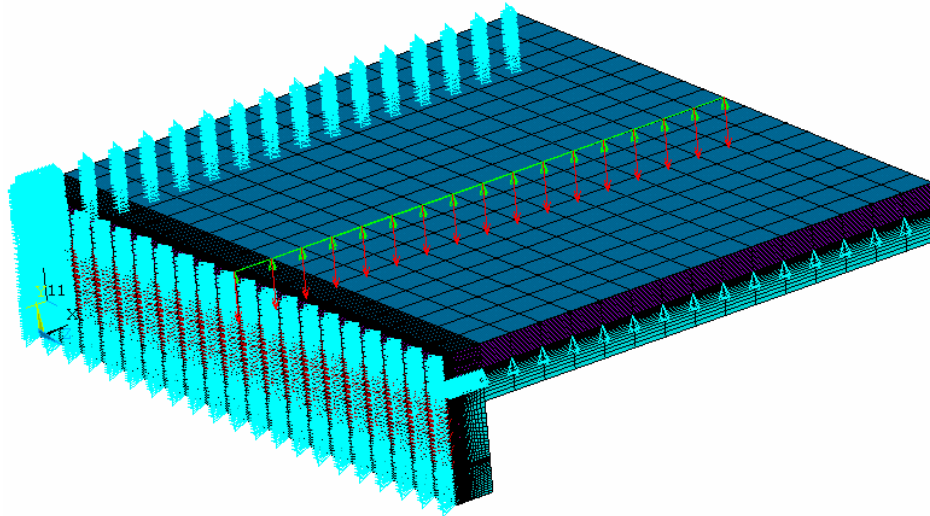


Figure 11. Boundary conditions for the structural FE-solution.

The FE model is solved as an elastic problem. It does not handle effects such as debonding of the GRP from the core material. This explains why the values from the FE-solution do not agree with the experimental data at elevated temperatures near T_g . Experimentally measured deflection is compared to the simulated in Fig. 12 with good agreement. The experimental data is provided by *Kockums*, from a 60 minutes fire test performed by *SP* [19].

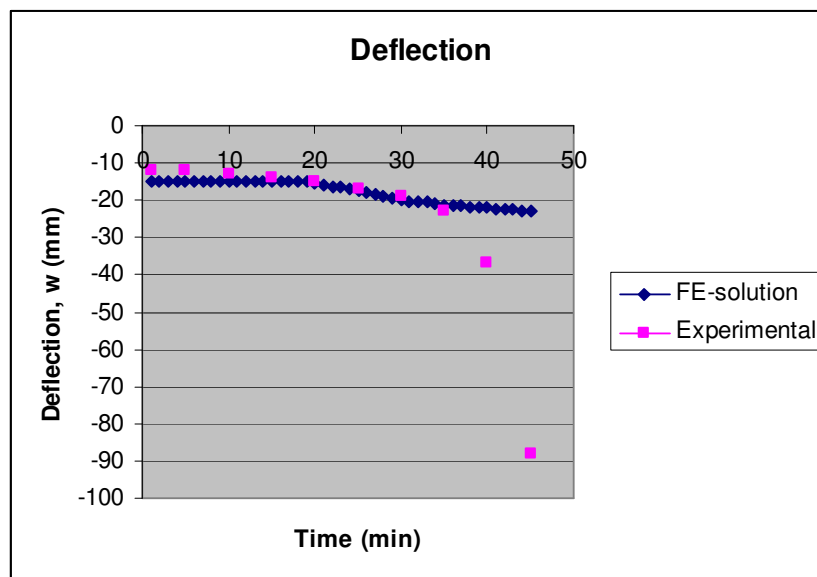


Figure 12. Measured and calculated deflection.

4.2. Failure load prediction tool

A tool for simple failure load estimations was created in Microsoft *Excel*. The aim was to have complementary software to the *Ansys* FE-analysis so that the degradation data quickly and easily can be used to estimate the failure load at any time step. One chapter is devoted to beam bending, where the deflection as a result of an applied out of plane force is calculated using beam bending theory. This is a common way to carry out a real life fire test and is therefore of interest.

4.2.1. Theory

The *Excel* tool automatically calculate failure load for a set of elementary load cases covering the most likely failure modes. Expressions of failure load are found in Ref. (20). The stress, σ , in the faces caused by bending moment are described by

$$\sigma_{f1} = -\frac{M}{t_1 d} \quad (8)$$

$$\sigma_{f2} = \frac{M}{t_2 d} \quad (9)$$

where M denotes moment, t face thickness and d the distance between face centres. Maximum moment before compressive failure in the upper face, f_1 , is

$$M_{\max} = -\sigma_{\text{comp}} t_1 d . \quad (10)$$

For simplicity in the *Excel* tool compressive modulus and strength are given as a positive number and therefore the expression used is

$$M_{\max} = \sigma_{\text{comp}} t_1 d . \quad (11)$$

Maximum moment before tensile failure in the lower face, f_2 , is

$$M_{\max} = \sigma_{\text{comp}} t_2 d . \quad (12)$$

Face wrinkling stress is given by

$$\sigma_f = 0.53 \sqrt{E_f E_c G_c} \quad (13)$$

where E_f and E_c is modulus of face and core respectively and G_c is the shear modulus of the core.

The maximum shear stress in the core is

$$\tau_{c \max} = \frac{T_x}{d} \quad (14)$$

Consider a simply supported panel as in Fig. 13. The panel is supported on all edges and a uniformly distributed load q (N/m²) is applied with a positive value downward. Face 1 denotes the upper face which will be subjected to compressive stress while the lower, face 2, will be subjected to tensile stress by bending.

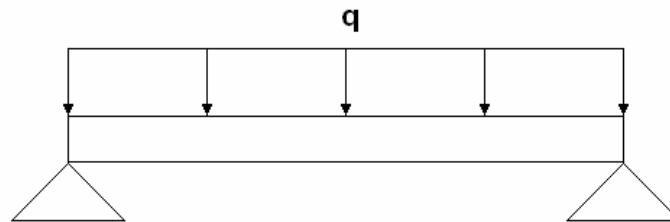


Figure 13. Simply supported beam subjected to a uniform load.

Moment in the panel is described as

$$M(x) = qLx - \frac{qx^2}{2} \quad (15)$$

which has a maximum at $x=L/2$, and since failure will occur at this maximum the equation is rewritten as

$$M(L/2) = M = \frac{qL^2}{8} \quad (16)$$

solving for failure load q

$$q = \frac{8M}{L^2} \quad (17)$$

The transverse force is described by

$$T_x = R_L - qx = \frac{qL}{2} - qx \quad (18)$$

which has a maximum

$$T_{\max} = T(0) = -T(L) = \frac{qL}{2} \quad (19)$$

Equations (17) and (19) together with equations (11), (12) and (13) gives us a set of failure loads for all failure modes, in which the lowest will be the designing value.

Now consider a simply supported panel with a point load at the centre of the plate as shown in Fig. 14. This is quite similar to the case above but the fact that the load is concentrated to the centre, produces a higher maximum bending moment in the panel.

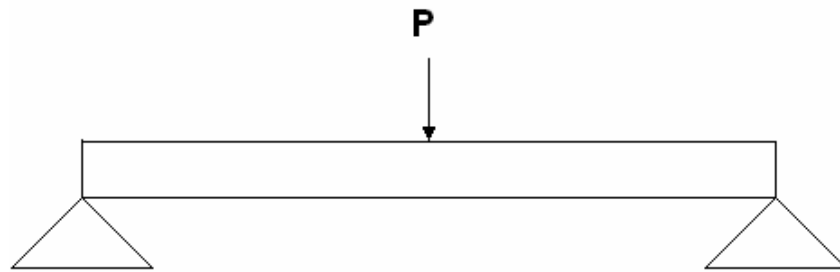


Figure 14. Simply supported beam subjected to a point load at the centre.

Moment in the panel is described as

$$M(x) = \frac{PLx}{2}, \quad 0 < x < L/2 \quad \text{and} \quad (20)$$

$$M(x) = \frac{PL(L-x)}{2}, \quad L/2 < x < L \quad (21)$$

which has a maximum at $x=L/2$, and since failure will occur in the maximum the equation is rewritten as

$$M(L/2) = M = \frac{PL^2}{4} \quad (22)$$

solving for failure load P

$$P = \frac{4M}{L^2} \quad (23)$$

The core failure load is calculated in the same way as in case with the uniform load, that is

$$T_{\max} = \pm \frac{PL}{2}. \quad (24)$$

Equations (23), (24) together with equations (11), (12) and (13) gives us a set of failure loads for all failure modes in which the lowest will be the designing value.

The third case is a panel with clamped edges and a uniformly distributed load, q (N/m²), acting on the top surface, see Fig. 15.

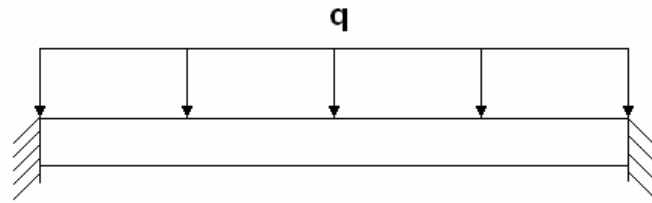


Figure 15. A panel with two clamped edges and a uniformly distributed load, q .

The moment in the panel is described as

$$M(x) = \frac{q}{2} \left(Lx - x^2 - \frac{L^2}{6} \right) \quad (25)$$

which has maximums at the clamped edges, that is

$$M = M(0) = -M(L) = \frac{qL^2}{12}. \quad (26)$$

And solving failure load, q ,

$$q = \frac{12M}{L^2} \quad (27)$$

The transverse force is described as

$$T(x) = \frac{q}{2}(L - 2x) \quad (28)$$

which has a maximum at

$$T_{\max} = T(0) = -T(L) = \frac{PL}{2} \quad (29)$$

Equations (27) and (29) together with equations (11), (12) and (13) gives us a set of failure loads for all failure modes, in which the lowest will be the designing value.

The fourth case is a panel subjected to a buckling force in both x and y-direction as seen in Fig. 16. The critical buckling load is calculated with Euler buckling. Other possible failure modes are face wrinkling and shear crimping of the core.

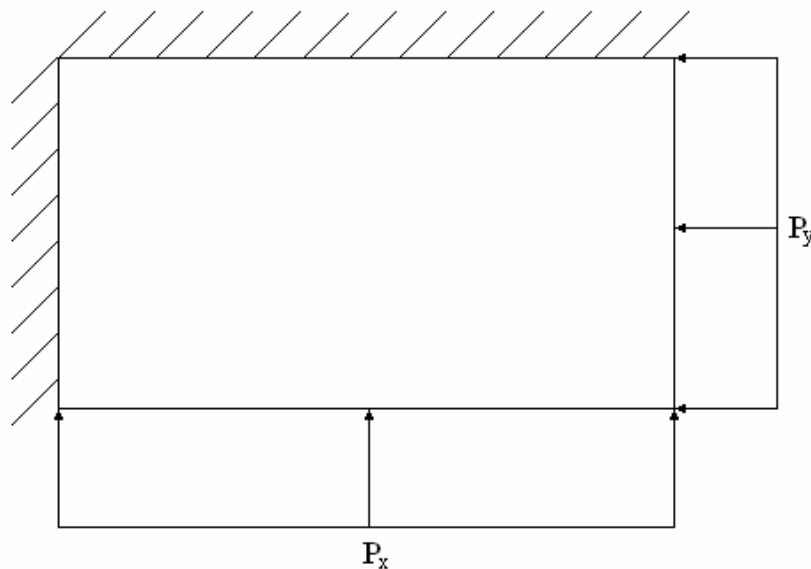


Figure 16. Panel subjected to buckling loads.

Euler buckling:

$$P_b = \frac{n^2 \pi^2 D}{\beta L} \quad (30)$$

In the buckling analysis of sandwich structures the transverse shear deformations must be accounted for as

$$\frac{1}{P_{cr}} = \frac{1}{P_b} + \frac{1}{P_s} \quad (31)$$

where

$$P_s = \frac{G_c d^2}{t_c}. \quad (32)$$

The face wrinkling stress is described as

$$\sigma_f = \frac{\sqrt[3]{E_f E_c G_c}}{2}. \quad (33)$$

Assuming that the two faces deforms the same gives

$$P_w = \frac{\sqrt[3]{E_f E_c G_c}}{2} \times (t_1 + t_2) \quad (34)$$

where t_1 and t_2 denotes the thickness of each skin.

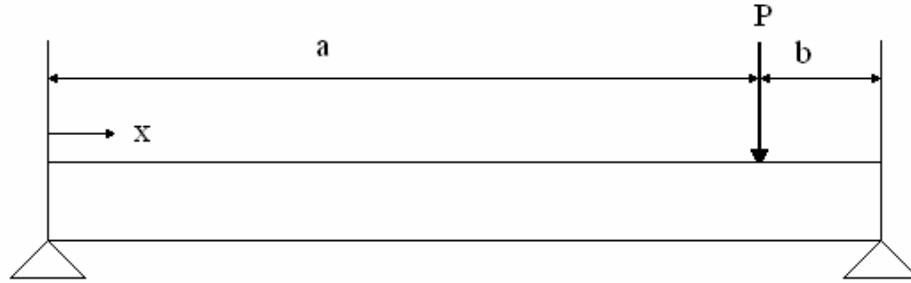


Figure 17. Simply supported beam subjected to a point load.

The deflection of a simply supported beam with an out of plane force as shown in Fig. 17 is described as

$$w_b = \frac{PL^3b}{6EI} \left[(1-b^2) \left(\frac{x}{L} \right) - \left(\frac{x}{L} \right)^3 \right] \quad (35)$$

where P is the force, L the beam length, and x is a local coordinate. In case of two forces the deflection will be the sum of the deflection caused by each force and if the forces are equal and symmetrically applied it can be written as

$$w_b = \frac{2PL^3b}{6EI} \left[(1-b^2) \left(\frac{x}{L} \right) - \left(\frac{x}{L} \right)^3 \right] \quad (36)$$

EI for a sandwich structure with thin faces and weak core is described as

$$EI = \frac{E_1 t_1 E_2 t_2 d^2}{E_1 t_1 + E_2 t_2} b_s \quad (37)$$

where d is the distance between the centres of the two faces. E denotes elastic modulus, t the face thickness, and b_s the beam width [21].

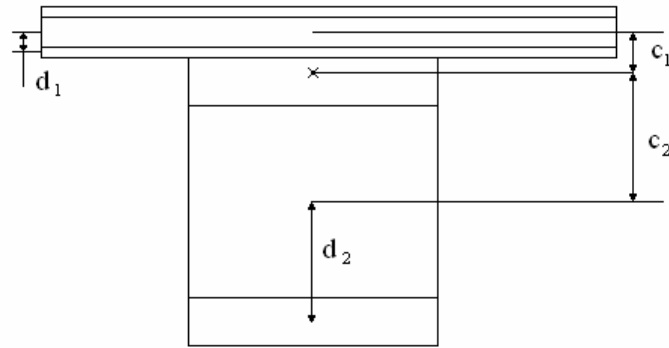


Figure 18. Stiffener attached to a sandwich panel.

When two structures are bonded together as shown in Fig. 18 the total bending stiffness becomes

$$EI = EI_1 + EI_2 + A_1 E_1 d_1 + A_2 E_2 d_2$$

where d_1 and d_2 denotes the distance between the bending centre of the separate parts and the bending centre of the combined structure. d_1 and d_2 can be derived from the relationship between the two parts. If one has a higher stiffness, the bending centre will move closer to that structures bending centre. As

$$\frac{c_1}{c_2} = \frac{EI_2}{EI_1} \quad (38)$$

but

$$c_1 + c_2 = d = \frac{d_1 + d_2}{2} \quad (39)$$

So c_1, c_2 can be rewritten as

$$c_1 = \frac{d_1 + d_2}{2} \frac{EI_2}{EI_1} \quad (40)$$

And

$$c_2 = \frac{d_1 + d_2}{2} - c_1 \quad (41)$$

The deflection caused by shearing is assumed to be negligible.

The *Excel* tool consists of two parts. First is failure load prediction, where material data is entered as input and the output is the load at which the structure will fail. The output is presented in a matrix with failure loads for several failure modes. This makes it easier to optimise the design for all failure modes, avoiding sub-optimising. The second part handles a specific case with a sandwich panel supported at two edges as described in 4.2.3. Here the output is the deflection caused by an out of plane load.

4.2.2. Procedure

Elastic properties for the sandwich faces must be calculated through micro mechanics and lamina theory. There are several softwares available for this application. Elastic properties for the GRP faces and the core material are entered as input data in the *Excel* document. Output from the *Excel* tool is deflection in beam bending and a predicted failure load. With thermal data from the fire simulations this can be repeated for each time step using the following set of conditions.

In room temperature the structure is intact and, in case of a stiffener as is the case addressed in this thesis, stiffness for the whole structure is calculated and used in the elastic predictions. However as the temperature in the GRP skin approaches T_g the face will start to debond from the panel and so a new bending stiffness must be calculated for a structure consisting of two parts, a separate laminate skin and a one-sided sandwich panel with a separate stiffener. At some point the stiffener will collapse due to core failure since it is exposed to the heat from two sides it will heat up quicker than the panel. The stiffeners GRP face is much thicker than the panels, therefore it will not separate from the core before the core reaches the softening temperature. Values for all three stages are displayed as output and it is up to the user to look in the thermal data to see which one is valid for each time step. Fig. 19 shows the different stages of failure

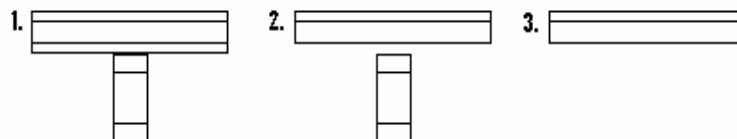


Figure 19. The three stages of failure. 1: intact sandwich structure with stiffener. 2: the hot face have separated from the core and has no contribution to the bending stiffness. 3: the stiffener collapses from core softening. Only a one sided sandwich remains which does not have much stiffness.

4.2.3. Simulation case 1

A simulation was made with a sandwich structure with a stiffener. The sandwich has glass fibre reinforced plastic, GRP, faces which are 2 mm thick where the matrix is a polyester resin with a T_g of 75 °C. The core is a 60 mm thick PVC foam with an expected softening temperature of 90 °C. The stiffener is built up as a sandwich structure which is narrow and high. Here the faces are 8.7 mm thick and the core is 220 mm. The whole structure is covered with 80 mm thick fire insulation. The experimental data is provided by *Kockums*, from a fire test performed by *SP*.

The structure is loaded with two out of plane forces which are applied at 25 % of the panel length from the edges. The forces are evenly distributed across the width as two bands. The panel is simply supported on two edges, the other two are free. The heat source follows an IMO fire curve. The temperature distribution in the fire insulation calculated in *Com Fire* is shown in Fig. 20. All temperatures are calculated as temperature increase from 18 °C room temperature.

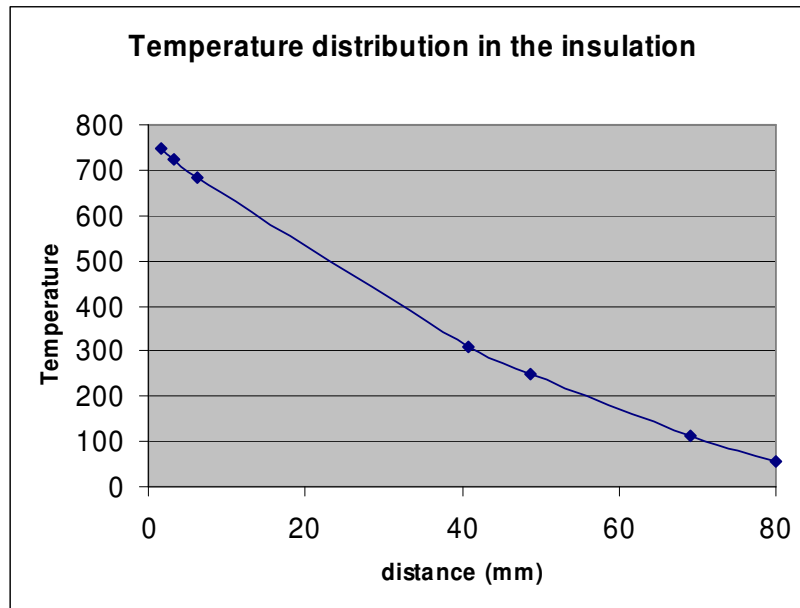


Figure 20. The temperature distribution in the insulation layer 30 minutes into the fire exposure.

The temperature on the cold side of the insulation is carried over to *Csp Fire* as boundary conditions for the thermal simulation of the sandwich structure. In Fig. 21 and 22 the temperature distribution is shown in the GRP and the core.

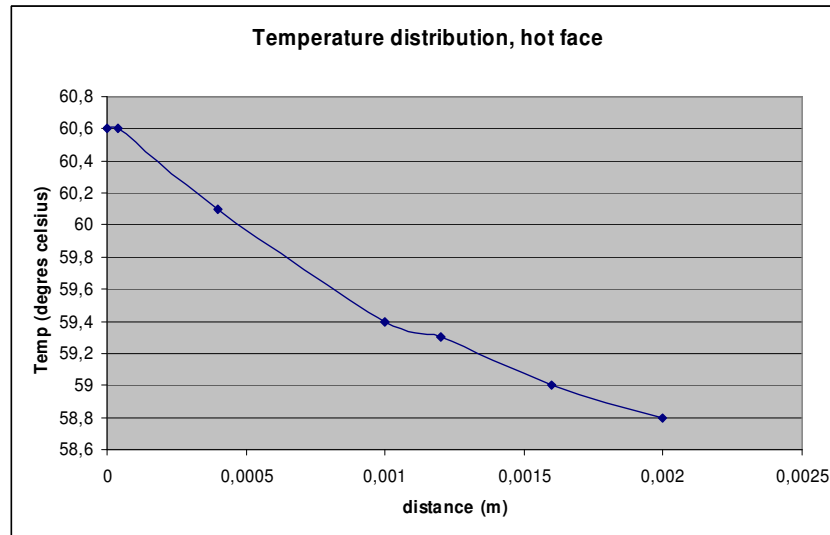


Figure 21. Temperature distribution in the hot face 30 minutes into the fire exposure. Notice that the temperature variation in GRP is small.

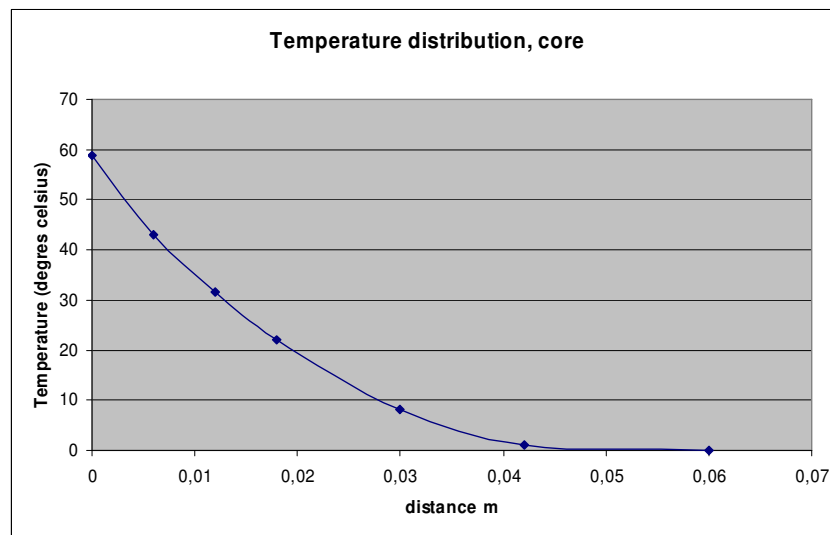


Figure 22. Temperature distribution in the core 30 minutes into the fire exposure. Notice that the temperature variation in GRP is small.

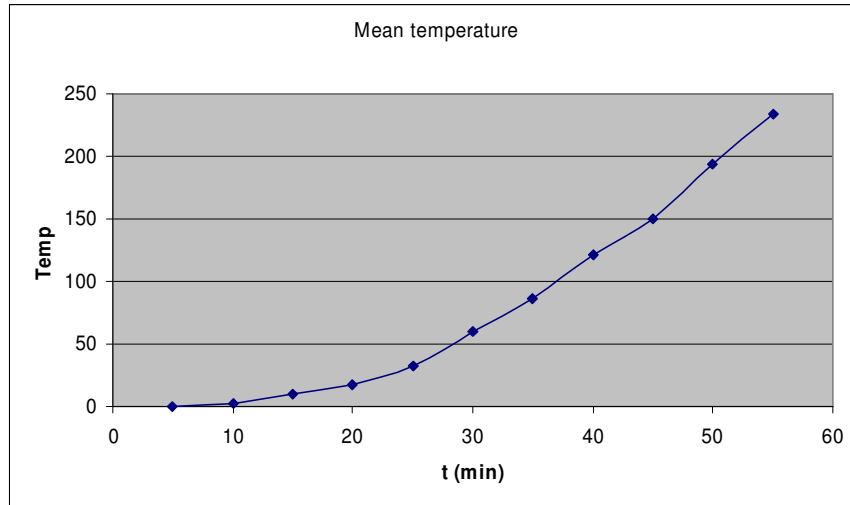


Figure 23. The mean temperature rise in the hot face GRP.

Just over 30 minutes into the fire test the hot face reaches near T_g , see Fig. 23, that is the temperature when the matrix loses load carrying capability. The face will separate from the sandwich structure with a big loss of stiffness. After 45 minutes the temperature in the core of the stiffener has reached such temperature that it collapses. In Fig. 24 the predicted and measured deflection is plotted. The *Excel* calculations seems to have predicted the main phenomena correctly.

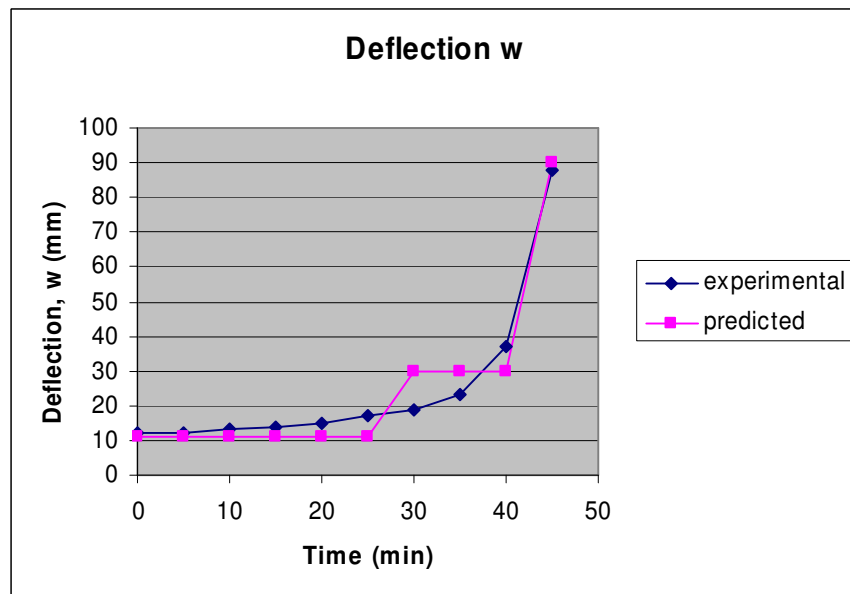


Figure 24. Experimental values plotted against the predicted. The three stages can be seen in the predicted deflection, undamaged structure, hot face separation and the stiffener collapse.

5. Failure Load Predictions of Composite Structures during Fire

Predicting how composites structures will behave in fire is important since they are used in critical applications such as load carrying structures. This chapter explains how and why the materials degrade and how its response can be predicted.

5.1. Material Degradation

All materials soften at elevated temperatures. However fiber/polymer composites degrade at a much lower temperature than metals, such as steel.

5.1.1. Fiber

The temperature at which degradation of the fiber reinforcement is initiated, around 400 °C, is reached long after the matrix has lost all structural integrity and is therefore not included in this model for material degradation.

5.1.2. Matrix

The matrix starts to degrade at an elevated temperature of about 200 °C, when mass loss starts to occur. However as it reaches T_g it has already lost about 99 % of its elastic properties as well as the corresponding strength. The degradation of the elastic properties is gradual until it reaches a temperature near T_g when the stiffness plunges dramatically down to about 1 % of the properties at room temperature. This fact is used to describe the softening of the structure. The glass transition temperature is the point at which the matrix material softens. Polyester and vinylester are widely used resins and have quite low T_g , typically ~75-100 °C. Epoxy resins can have a T_g of around ~120-150 °C and phenolic resins can have a T_g even over 150 °C.

Polyester, vinylester and epoxy degrade in a similar way. At elevated temperatures mass loss begins to occur as a result of the polymer chains degrades and escapes as gases. The thermal responses to the fire degradation of these three resins are nearly identical and simulation conclusions made from simulations are principally valid for all three. Phenolic resins form a layer of char as it degrades which acts as a thermal barrier, making it more fire resistant. It is assumed that when the remaining mass get below 80 % the material will have started to form char and lost its elastic properties, [15].

5.1.3. Core Material

Commonly used core materials are foam such as PVC or PU and balsa wood. The foam will lose all stiffness when the temperature increases up to the point of collapse. This temperature is typically below 100 °C. Balsa wood is more temperature resilient and will soften in temperatures over 200 °C.

5.2. Failure Hypothesis

Several phenomena occur in the material during fire at elevated temperatures. A failure hypothesis, according to the weakest link theory, has here been assumed regarding known phenomena which affects the material's structural behaviour. The following phenomena are considered:

1. Thermal degradation of the matrix material:

When the matrix in the GRP skin reaches T_g the matrix softens because of changes in the molecular structure. The matrix modulus is typically reduced with a factor of 100 for temperatures above T_g . The effect on the strength of the GRP skin is depending on the stress state (compressive or tensile load). Tensile strength is reduced much less than compressive strength. The hot face laminate in many constructions will have local or global compression stresses and hence a low strength, for temperatures above T_g .

2. Fire degradation of the matrix material:

If there are fire induced degradation effects in the matrix the elastic properties are assumed to stay unchanged until the remaining resin content, *RRC*, reaches 90 %. It is assumed that this will never be the cause of failure since the GRP normally reaches T_g well before degradation of the matrix starts. However in structures that have been subjected to fire and are loaded after cooling, degraded matrix would probably be considered as a likely cause of failure.

3. Thermal degradation of the laminate/core interface:

The shear strength of the laminate/core interface is controlled by the T_g of the matrix and the softening temperature of the core material. This shear strength is hence assumed to be negligible for temperatures above T_g or above the core softening temperature. If an adhesive film is used to bond the GRP and core and has a lower T_g than the GRP this will be the weakest link since it will have the same temperature as the GRP.

4. Thermal degradation of the core material:

When the core temperature rises it will soften. Foam cores will lose stiffness gradually until the point when all structural stability is lost. Balsa wood has higher thermal stability and will lose all structural stability around 200 °C while foam cores lose stability at around 90-120 °C.

Phenomena Nr 2 can normally be neglected for failure predictions of composites during fire, since phenomena Nr 1 already reduces stiffness and strength significantly. This is likely to be especially true for structures which have a separate fire insulation, which suppresses fire degradation in the structure and lowers the temperatures. Thermal degradation phenomena Nr 1, 3 and 4 are hence assumed to control significant loss of strength and stiffness of the structure according to the weakest link theory.

5.3. Composite Structure with Fire Insulation

Load carrying structures that are used in an environment where it could be exposed to fire, are commonly protected with fire insulation, e.g. mineral wool.

5.3.1. Procedure

The procedure involves three steps. First the temperature distribution through the structure must be calculated. The second step is to simulate the material degradation due to the raised temperature. With the temperature distribution known a structural analysis can be done using the *Excel* tool. Because of limitations in the *Com Fire* and *Csp Fire* software the fire simulation must be done in three steps. First a simulation of the temperature distribution through the fire insulation layer must be made in *Com Fire*, from which the boundary conditions for the two following steps are extracted. The next step is to calculate the temperature distribution through the entire sandwich structure using *Csp Fire*. The last step is to run a full analysis including matrix degradation in the hot face GRP. This has to be done separately in *Com Fire* since *Csp Fire* does not seem to handle the fire degradation properly. The structural analysis is carried out in the *Excel* tool. The mean temperature in the GRP is used from the thermal analysis. If the relation between stiffness and temperature is known for the matrix, the elastic properties can be recalculated for each time step. Such data can be hard to acquire. In that case the stiffness of the GRP skin is set to zero when temperature reaches near T_g .

5.3.2. Parameter Study

The effect of the fire degradation (material fire kinetics model) on the thermal analysis is investigated by simulating two cases of GRP panels subjected to fire. A polyester matrix is used in the simulation and the indicated conclusions would also be valid for vinylester and epoxy since their fire response are very similar. The cases are simulated with and without the degradation effect included, with 30 and 50 mm insulation and the results from the simulations are shown in Fig. 25. The thermal effects are shown to be negligible at the relatively low temperatures where fire insulation is used and is not necessary to include in such simulations. A 5 mm thick glassfiber reinforced panel with a fiber volume fraction of 0.54 and the heat source follows an IMO fire curve.

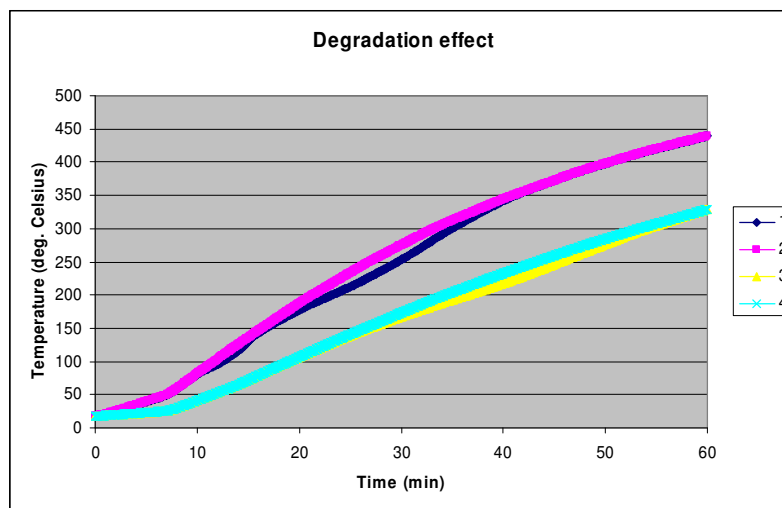


Figure 25. Temperature in node 31/51 in a 60 minute fire simulation on a GRP plate protected by 50 mm (1 and 2) and 30 mm (3 and 4) insulation respectively and fire degradation effects included (1 and 3) and excluded (2 and 4).

The effect of the fire degradation (material fire kinetics model) was also simulated for a phenolic resin. The effect of charring was not included in the simulation and this is expected to have a large influence on the thermal conductivity and the simulation parameters for the simulation are hence not reliable. Result of the simulation is shown in Fig. 26. A 5 mm thick glassfiber reinforced panel with fiber volume fraction of 0.54 where the heat source follows an IMO fire curve, was simulated. The fire degradation influence on the temperature response of this laminate is negligible.

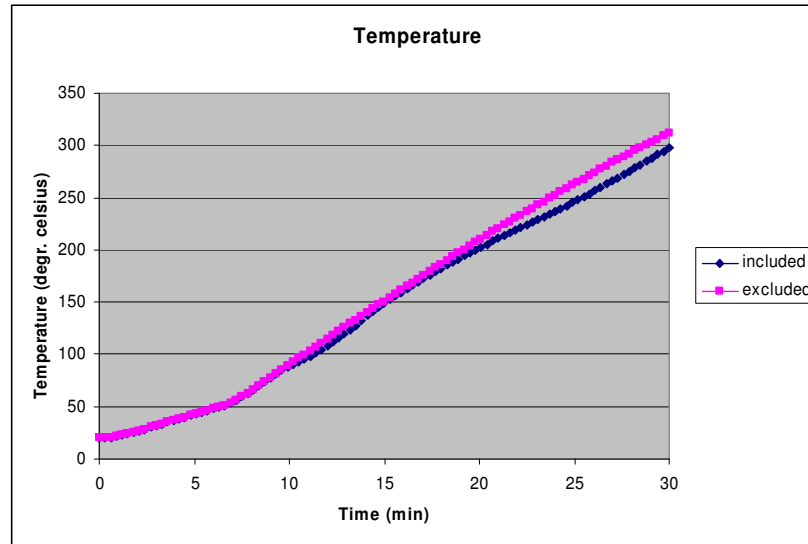


Figure 26. The temperature in node 21/51 in the phenolic GRP.

In a sandwich with thin faces and a foam core the GRP has much higher thermal conductivity than the core which acts like an insulation on the cold side of the hot face. When fire insulation is used the relatively slow heating process results in a very small temperature difference through the thickness of the GRP. In Fig. 21 the temperature difference is no more than 2 °C. It is assumed that the temperature can be treated as constant through the thickness of the GRP in the mechanical analysis. The temperature difference in the core gets large because of the low thermal conductivity. However the interface between the core and the GRP will always be the same temperature. This fact justifies the assumption that the core and GRP should have similar softening temperature, or at least the lowest will be the designing temperature.

The Glass transition temperature T_g is important in the thermal mechanical analysis and design as it is the point where the matrix loses structural integrity. The time when the matrix in the hot face reaches T_g for resins with differing T_g ranging from 60-150 °C, are shown in Fig. 27. The sandwich structure has 2 mm glass fibre reinforced polymer faces and a 60 mm thick core. The structure is insulated with 80 mm mineral wool and subjected to an IMO fire curve.

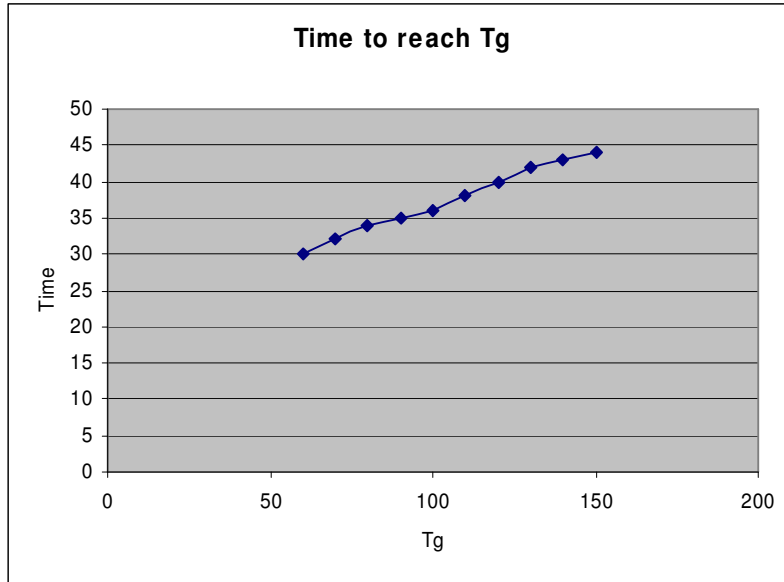


Figure 27. Time to reach Tg in the hot face GRP.

Another important part is the thickness and thermal properties of the fire insulation. In Fig. 28 the time to reach 75 °C can be seen. A 5 mm thick glassfiber reinforced panel with a fiber volume fraction of 0.54 and the heat source follows an IMO fire curve.

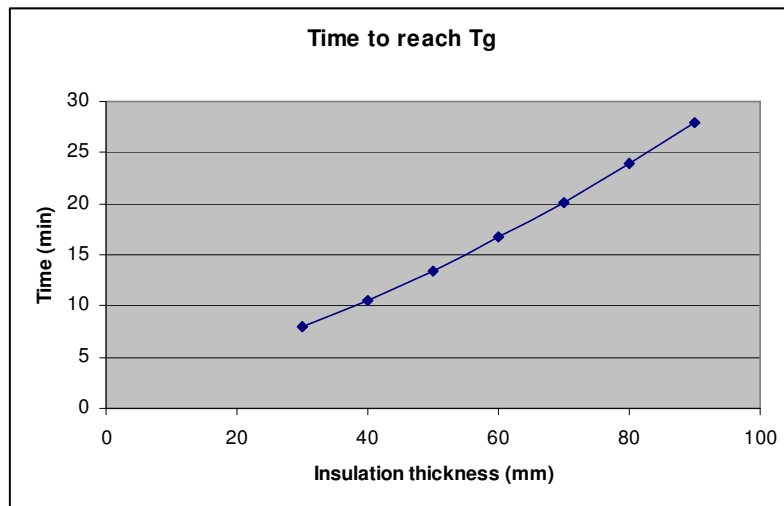


Figure 28. Time until the surface of the GRP reaches 75 °C with varying thickness of the insulation.

A simulation was made with the panel from chapter 4.2.3, case 1. The difference is the materials used. A phenolic resin with T_g of 200 °C is used instead of polyester with a T_g of 75 °C and a balsa wood core instead of the PVC core. The balsa is assumed to loose stiffness and strength with a factor of 100 when it reaches 200 °C. The balsa wood has a much higher thermal conductivity than the foam core and because of this the temperature in the GRP will be a little lower in case 2, see Fig. 29. However the difference is too small to be of any significance. This case is referred to as case 2. All temperatures are calculated as temperature increase from 18 °C room temperature.

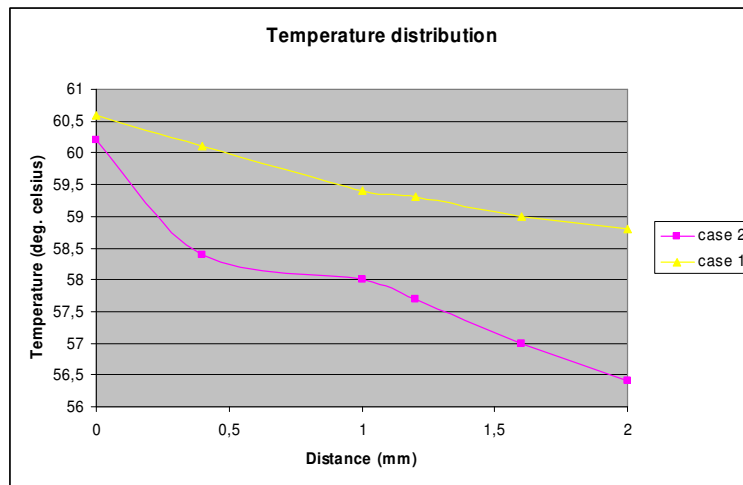


Figure 29. Comparison between the temperature distribution in the hot face in case 1 and 2.

The temperature distribution in the core can be seen in Fig. 30.

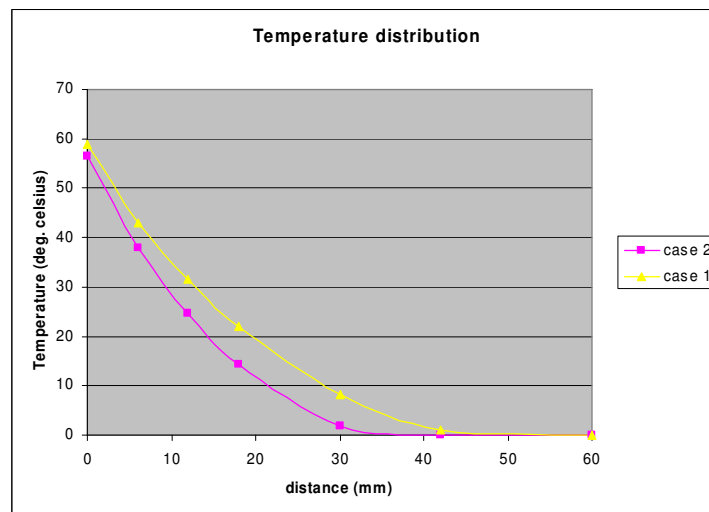


Figure 30. Temperature distribution in the core material 30 minutes into the fire exposure in case 1 and 2.

In this case 2 the temperature will reach the point of softening in the stiffener core after 47 minutes and will lose all load carrying capability. The temperature in the faces of the panel at this time is close to T_g . The panel will not be able to take all the load without the stiffener and the entire structure would collapse in a fast course of events. A comparison between the events of case 1 and 2 is shown in Fig. 31.

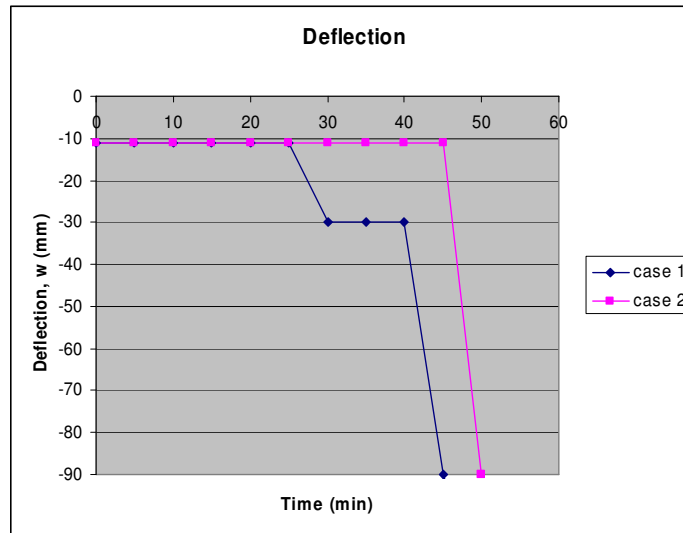


Figure 31. Deflection caused by a load on a sandwich structure exposed to fire.

Simulations were also made on case 1 with 50 and 90 mm insulation layer. Except for insulation thickness the material properties are identical to case 1, described in section 4.2.3. The effect of fire insulation on the time to failure is shown in Fig. 32.

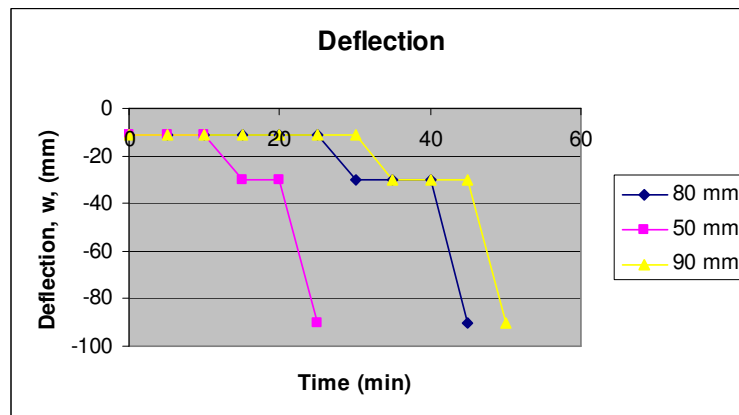


Figure 32. The deflection of loaded panels subjected to the same load and heat source with 50, 80 and 90 mm fire insulation.

5.3.3. Summary

The results from chapter 5.3.2. are summarised in Tab. 1 and an estimation of the influence is shown in Tab. 2.

Table 1. Summary of the parameter study.

Parameter	Value	Time of initial failure
Insulation thickness	50 mm	12 min
Insulation thickness	80 mm	27 min
Insulation thickness	90 mm	33 min
Tg	75 °C	33 min
Tg	100 °C	36 min
Tg	150 °C	44 min
Kinetic thermal model	excluded	27 min
Kinetic thermal model	included	27 min

Table 2. The parameter influence on the thermal analysis.

Parameter	Influence
Thermal model pe, ve, ep	very low
Thermal model phenol	very low
Tg	medium
Insulation thickness	high

5.4. Composite Structure without Fire Insulation

The effect of the fire exposure on an unprotected GRP is more intense, without fire insulation protecting the structure. This means that the temperature distribution is more differentiated and degradation of the matrix must be taken into consideration within the time to failure.

5.4.1. Procedure

The procedure is quite similar to the case with insulation but without the first step. Fire simulation is first carried out in *Csp Fire* for the sandwich structure, not including degradation effects. Another simulation is carried out in *Com Fire* with the degradation effects included. Then a comparison between the two sets of results must be done, to show if the degradation process has a large influence on the temperature distribution. If not, the effects are neglected and the temperature distribution is taken from *Csp Fire* and the degradation depth from *Com Fire* but in case the effect is not negligible one can try to alter some of the parameters in *Csp Fire* to adjust the results to *Com Fire*. In case it isn't a sandwich but just a GRP it is only necessary to run the simulations in *Com Fire*.

The structural analysis is carried out in the *Excel* tool. The mean temperature in the GRP is used from the thermal analysis. At every time step, the depth where degradation is higher than the predetermined value and the depth at which the temperature is near T_g must be calculated from the output data, and an effective thickness is derived by reducing the virgin thickness with the larger of the two. A suitable value for acceptable matrix degradation is 10 % (90 % RRC) before the material is expected to lose elastic properties and starts to form char.

5.4.2. Parameter Study

The two most important factors determining the time to failure for a composite material exposed directly to fire without insulation is the amount of material degradation as well as the glass transition temperature, T_g . In Fig. 33 the remaining resin content are shown for different resins through the exposure time. Polyester and vinylester degrades at a similar rate while the epoxy resin degrades faster. A 5 mm thick glassfiber reinforced panel with a fiber volume fraction of 0.54 where the heat source follows an IMO fire curve was simulated.

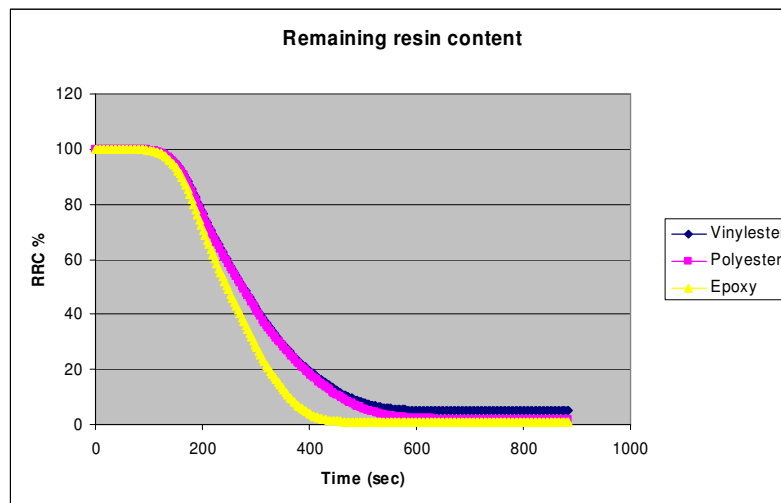


Figure 33. Remaining resin content for three common resin systems. In all three cases a 5 mm thick panel is subjected to a HC-fire curve.

The cooling effect of the endothermic degradation process is shown in Fig. 34. The temperature is simulated with and without the degradation effect included. The largest temperature difference is about 100 °C. However this effect only gets influential at temperatures above T_g . No reliable data was acquired for degradation parameters for the phenolic resin so the result should not be considered as valid. A 5 mm thick glassfiber reinforced panel with a fiber volume fraction of 0.54 where the heat source follows an IMO fire curve was simulated.

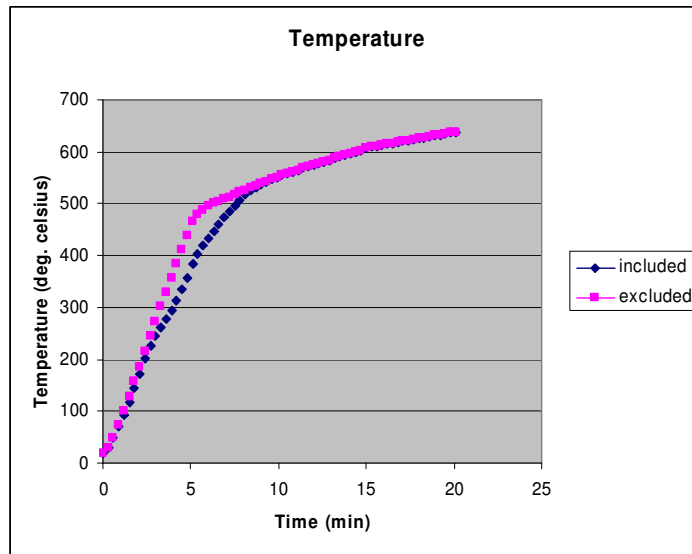


Figure 34. Temperature at node 26 for a phenolic composite simulated with and without fire degradation effect included.

When the remaining resin content is 80 % the resin is assumed to loose the majority of its elastic properties. In Fig. 28 the depth of the damaged material is shown for the same case as in Fig. 35.

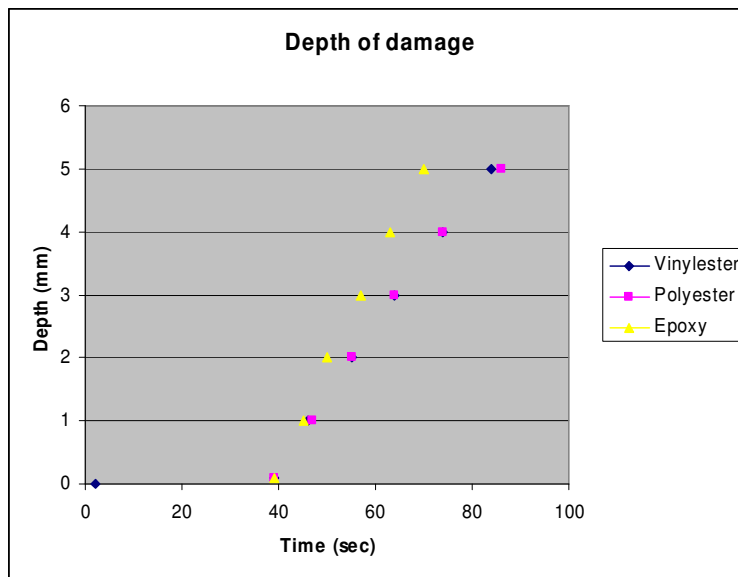


Figure 35. The depth where the degradation has reached 20 %.

It is noticeable that a layer of insulation prolongs the time to failure dramatically as can be seen in Fig. 36. The time needed to reach T_g is over 10 times as long when the GRP is insulated with 50 mm thick mineral wool. It is shown that to improve the time to failure adding fire insulation is a more effective tool than raising the resin T_g . By raising T_g 125 °C from 75 to 200 °C the increase in time until the mean value reaches this temperature is 90 s. The increase of time until the temperature reaches T_g of a fire insulation as thin as 30 mm is about 510 s. A combination of raising the T_g 50 °C and protecting the structure with 30 mm fire insulation increases this time with just over 750 s. Note that the effect of fire insulation on the time to failure is much larger than a raised T_g , however a raised T_g has much larger effect in combination with insulation than without. A 5 mm thick glassfiber reinforced panel with a fiber volume fraction of 0.54 and the heat source which follows an IMO fire curve was considered.

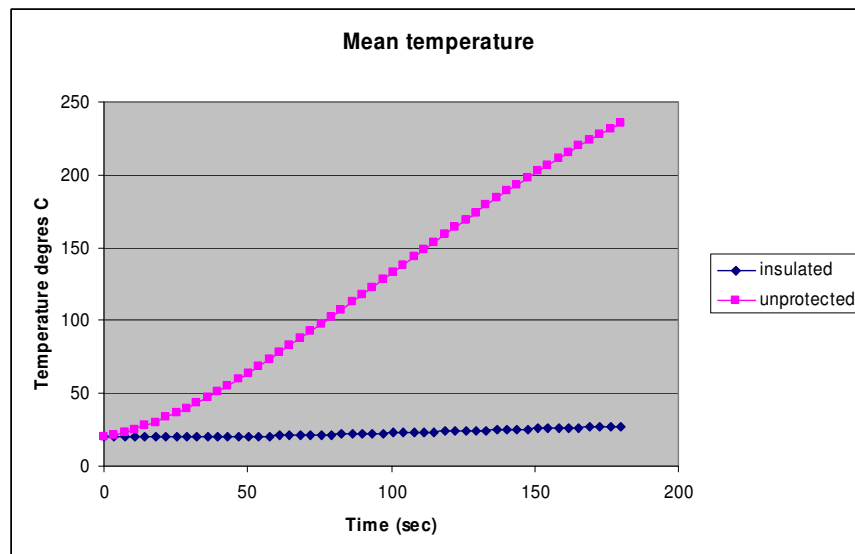


Figure 36. The mean temperature in the unprotected GRP and with 50 mm insulation.

6. Conclusions

It is shown that to some extent the material degradation can be predicted. The method presented in this work is a usable tool in the design of composite structures which requires fire safety. The fundamental mechanisms of failure are addressed. Such as a large loss of stiffness in the matrix at temperatures near T_g and the collapse of the core when foam materials are used in the core. Balsa wood will lose its stability at a higher temperature and might be more suited to structures exposed to fire.

Although there are some good software available for simulating the degradation of the resin it is suggested that focus should be laid on simulating the heat transfer and the softening of the resin as it reaches T_g . The reason is that in applications where a load carrying structure is used with a demand on fire safety, the composite structure is usually protected by a layer of fire insulation. This means that the structure will be heated up slowly and it will collapse from loss of stiffness when it reaches T_g before any degradation and mass loss of the resin have commenced. If post-fire mechanical properties are of interest, a degradation simulation is vital to perform. This could be of interest if the heat exposure time is short and estimations of the load bearing capabilities in a post-fire after fire must be considered.

Important material properties for fire safety design are the thickness and thermal properties of the fire insulation and the softening of the resin at elevated temperatures. Choosing a resin with a high T_g and a sufficient insulation can save several minutes of structural integrity. Insulating has largest effect but a combination of fire insulation and raised T_g is most effective.

Structural calculations such as FE can be useful however an elastic approach to the problem means that the failure mechanism can be hard to simulate. In most cases a thermal analysis is sufficient and conclusions can be made by looking at the temperature distribution in the structure.

Usable measured data are hard to get on the subject. Fire tests are expensive to do and the results are seldom publicised. For a validation of the software and methods presented in this work more test data must be gathered from real life fire tests. Also the loss of elastic properties for resin at elevated temperatures should be investigated with thermo-mechanical testing.

7. Acknowledgements

I would like to thank Kurt Olofsson at Sicomp and Roberts Joffe at Luleå University of Technology for their support. I would also like to thank Henrik Johansson at Kockums for providing me with useful experimental data and Prof. A.G. Gibson for providing software and material data.

8. References

1. Lay F. and Gutierrez J. “*Improvement of the Fire Behaviour of Composite Materials for Naval Application*”, Elsevier, France, (1997)
2. Ming Dao and Asaro J., “*Fire Degradation of Fiber Composites*”, Marine technology, USA, (1997)
3. Ming Dao and Asaro J., “*A study on Failure Prediction and Design Criteria for Fiber Composites under Fire Degradation*”, Elsevier, USA, (1998)
4. Mouritz A.P. and Mathys Z., “*Post-Fire Mechanical Properties of Glass-reinforced Polyester Composites*”, Elsevier, Australia, (2000)
5. Kwon S.W., Smith W.L. and Lee S.W., “*Thermo-viscoplastic Modelling of Composites Exposed to Fire or High Temperature*”, Journal of Composite Materials, USA, (2006)
6. Blasi C and Branca C, “*Mathematical Model for the Nonsteady Decomposition of Intumescent Coatings*”, AIChE Journal, Italy, (2001)
7. Birman V. Kardomateas G.A., Simitzes G.J. and Li R., “*Response of a Sandwich Panel Subject to a Fire or Elevated Temperature on one of the Surfaces*”, Elsevier, USA, (2006)
8. Lyon R. E., Balaguru P. N., Foden A., Sorathia U., Davidovits J. and Davidovics M., “*Fire-resistant Aluminosilicate Composites*”, Fire and Materials, USA, (1997)
9. Mouritz A.P. and Mathys Z., “*Mechanical Properties of Fire-damaged Glass-reinforced Phenolic Composites*”, Fire and Materials, Australia, (2000)
10. Hergenrother P.M., “*Flame Retardant Airplane Epoxy Resins Containing Phosphorous*”, Elsevier, USA, (2005)
11. Mouritz A.P., “*Ballistic Impact and Explosive Blast Resistance of Stitched Composites*”, Elsevier, Australia, (2001)
12. Cogging J.M., “*Response of Isotropic and Laminated Plates to Close Proximity Blast Loads*”, USA, (2000)

13. Park H., Lee K., Lee S.W. and Kim K., “*Dynamic Analysis of Nonlinear Composite Structures under Pressure Wave Loading*”, Journal of Composite Materials, USA, (2005)
14. Ashley S., “*Safety in the Sky: Designing Bomb-resistant Baggage Contain*”, Mechanical Engineering, USA, (1992)
15. Com Fire, version 4.1, University of Newcastle, UK, (2005)
16. Csp Fire, version 1.0, University of Newcastle, UK, (2005)
17. Gibson A.G., Wright P.N.H., Wu Y.-S., “*The Integrity of Polymer Composites During and After Fire*”, Journal of Composite Materials, UK, (2004)
18. ANSYS, release 10, ANSYS, Inc, US
19. Hilling R., “*Fire Test of a Loadbearing deck*”, SP Swedish National Testing and Research Institute, Sweden, (2006)
19. Zenkert D., “*Sandwich Construction*”, Engineering Materials Advisory Services Ltd,UK, (1997)
20. Sundström B., “*Handbok och Formelsamling i Hållfasthetslära*”, KTH, Sweden, (1999)